Structure and Orientation of the Transmembrane Domain of Glycophorin A in Lipid Bilayers†

Steven O. Smith*

Department of Molecular Biophysics and Biochemistry, Yale University, New Haven, Connecticut 06520-8114

Roy Jonas and Mark Braiman

Department of Biochemistry, University of Virginia School of Medicine, Charlottesville, Virginia 22908

Barbara J. Bormann

Boehringer-Ingelheim, Ridgefield, Connecticut 06877

Received December 3, 1993; Revised Manuscript Received March 10, 1994®

ABSTRACT: Rotational resonance (RR) NMR, circular dichroism (CD), and attenuated total reflection Fourier transform infrared (ATR-FTIR) spectroscopy are used to establish the secondary structure and orientation of peptides corresponding to the transmembrane domain of human glycophorin A in dimyristoylphosphatidylcholine bilayers. An amide I vibrational frequency of 1650 cm^{-1} and negative CD absorption bands at 208 and 222 nm indicate that the peptide is largely α-helical, while an order parameter of 0.35–0.50 in the ATR-FTIR measurements indicates that the peptide orientation is generally perpendicular to the bilayer plane. High-resolution structural data on the glycophorin A transmembrane (GPA-TM) peptides were obtained by measuring the rate of magnetization exchange between pairs of specific ^{13}C labels using RR NMR. The exchange rates are translated into internuclear distances with a resolution on the order of 0.3 Å. These experiments are similar in design to previous experiments on crystalline peptides where the ^{13}C labels were incorporated into amino acids separated by 2–3 residues in the peptide sequence but close together in space due to a helical peptide geometry [Peersen, O. B., Yoshimura, S., Hojo, H., Aimoto, S., & Smith, S. O. (1992) *J. Am. Chem. Soc. 114,* 4332–4335]. In the GPA-TM peptides, magnetization exchange rates measured between [1-^{13}C]V_{80} and [2-^{13}C]G_{83} and between [1-^{13}C]M_{81} and [2-^{13}C]G_{83} in the middle of the transmembrane sequence correspond to internuclear distances of ~4.5 Å and are consistent with a helical peptide structure. RR NMR measurements between [1-^{13}C]I_{91} and [2-^{13}C]-G_{94} also indicate a helical geometry; however, longer distances are observed between [1-^{13}C]I_{95} and [2-^{13}C]-G_{98} which argue that the transmembrane helix unravels at the membrane interface. These data demonstrate that high-resolution measurements of local protein structure can be made in lipid bilayers.

Integral membrane proteins generally span lipid bilayers in regular secondary structures to accommodate hydrogen bonding of the peptide backbone in a hydrophobic environment. The dominant motif in many membrane proteins appears to be the transmembrane α-helix, and interactions between helices serve to stabilize the protein tertiary structure or drive protein oligomerization [see Bormann and Engelman (1992)]. Structural studies on such systems are hindered by the difficulty in obtaining crystals for X-ray diffraction and by restricted motion which makes them unsuitable for high-resolution solution NMR techniques. The global secondary structure of membrane proteins is often estimated from the circular dichroism (CD)[1] of the backbone amide absorption band or the amide I and II vibrational frequencies. Recently, rotational resonance (RR) NMR methods have been developed for obtaining information on the *local* secondary structure of a short hydrophobic peptide through the measurement of specific internuclear distances (Peersen et al., 1992; O. B. Peersen, S. Aimoto, and S. O. Smith, in preparation). These studies are extended in this paper to a peptide corresponding to the transmembrane (TM) domain of glycophorin A (GPA). The NMR results are combined with CD and attenuated total reflection Fourier transform infrared (ATR-FTIR) measurements to characterize the secondary structure and orientation of the GPA-TM domain in membrane bilayers.

Rotational resonance NMR is a magic angle spinning (MAS) based approach for obtaining internuclear distances through the measurement of weak homonuclear dipolar couplings (Raleigh et al., 1988; Levitt et al., 1990; Peersen & Smith, 1993). RR uses the MAS frequency to selectively restore the dipolar couplings that are averaged in a MAS experiment. The sample is rotated at a frequency ω_r such that $n\omega_r = \Delta\omega$, where n is a small integer and $\Delta\omega$ is the difference in isotropic chemical shifts of the dipole-coupled resonances. Specific ^{13}C labels are often used for RR NMR studies since ^{13}C has a wide chemical shift range and can be incorporated into peptide backbone and side-chain positions. RR NMR has been successfully applied to study the local conformation of the retinal chromophore in bacteriorhodopsin, an integral membrane protein that functions as a light-driven proton pump (Thompson et al., 1992; Farrar et al., 1993), and

† This research was supported by the National Institutes of Health (GM-41412), the American Cancer Society (BE-138), and the Searle Scholars Program/Chicago Community Trust to S.O.S. and by the National Science Foundation (CHE-8907991) and the Whitaker Foundation to M.S.B.

* To whom correspondence should be addressed.

® Abstract published in *Advance ACS Abstracts,* April 15, 1994.

[1] Abbreviations: ATR-FTIR, attenuated total reflection Fourier transform infrared; CD, circular dichroism; DMPC, dimyristoylphosphatidylcholine; GPA-TM, glycophorin A transmembrane; RR NMR, rotational resonance nuclear magnetic resonance spectroscopy; VACP, variable-amplitude cross polarization.

0006-2960/94/0433-6334$04.50/0 © 1994 American Chemical Society

the secondary structure in model hydrophobic undecapeptides in crystals and lipid bilayers (Peersen et al., 1992), where distances up to 6.8 Å have been measured between specific ^{13}C sites.

The transmembrane domain of glycophorin A provides an ideal model system for developing RR NMR for structural studies of membrane proteins and peptides. Glycophorin spans the cell membrane of erythrocytes with a single stretch of 23 mostly hydrophobic amino acids. The transmembrane domain boundary is marked by charged glutamate or arginine residues. Marchesi and co-workers have demonstrated that the transmembrane domain is responsible for dimerization of the protein (Furthmayr & Marchesi, 1976; Bormann et al., 1989) and on the basis of methyl carboxylation studies argued that M_{81} lies in the dimer interface. Recently, mutagenesis studies have revealed that conservative changes at G_{79}, V_{80}, G_{83}, and V_{84} in the transmembrane sequence disrupt dimerization, while dimerization is relatively tolerant of changes at M_{81} (Lemmon et al., 1992a,b). These results together with molecular modeling have suggested that the glycophorin transmembrane domain has a helical structure with G_{79} and G_{83} packed in the helix interface and M_{81} facing the lipid chains (Treutlein et al., 1992). One interesting finding of these studies was that the dimer appears to form a right-handed coiled-coil with a spacing of 3.9 residues per turn.

In this paper, we combine ATR-FTIR, CD, and RR NMR measurements to establish the secondary structure of the transmembrane domain of glycophorin A in lipid bilayers. The CD and polarized ATR-FTIR results indicate that the peptide is largely α-helical and oriented perpendicular to the bilayer plane. RR NMR measurements of specifically ^{13}C-labeled peptides are used to probe the local secondary structure along the length of the helix. Magnetization exchange rates measured between [1-^{13}C]V_{80} and [2-^{13}C]G_{83} and between [1-^{13}C]M_{81} and [2-^{13}C]G_{83} are consistent with an α-helical structure in the middle of the transmembrane sequence. The helical geometry extends through G_{94} but begins to unravel at the membrane interface. These measurements along with those of lipid–glycophorin interactions described in the preceding paper (Smith et al., 1994) illustrate the use of RR NMR to characterize local structure in membranes.

MATERIALS AND METHODS

The ^{13}C-labeled amino acids (99% enriched) were obtained from Cambridge Isotopes (Cambridge, MA) or Tracer Technologies (Cambridge, MA) as the *t*-Boc derivatives or as the free amino acids and were derivatized by standard methods (Roeske, 1963) at Boehringer Ingelheim (Ridgefield, CT). The GPA-TM peptides were synthesized at the Protein and Nucleic Acid Chemistry Facility at Yale University and were purified by reverse-phase HPLC on a semipreparative or preparative Vydac C4 column using an acetonitrile/2-propanol/water gradient. Crude lyophilized peptide was dissolved in 88% formic acid and loaded onto the column with a solvent mixture (v/v) of 70% water, 12% acetonitrile, and 18% 2-propanol. The mixture was changed in a single step to 20% water, 32% acetonitrile, and 48% 2-propanol, and then in a linear gradient to 40% acetonitrile and 60% 2-propanol. The peptide eluted near the end of the linear gradient. The sequence corresponds to the transmembrane region of human glycophorin A.

P-**E**-I-T-L-I-I-F-G-V_{80}-M_{81}-A-G_{83}-V-I-G-T-I-L-L-I_{91}-
S-Y-G_{94}-I_{95}-**R**-**R**-L(G_{98})-I

For the intramolecular RR NMR measurements, specific ^{13}C labels were incorporated at [1-^{13}C]V_{80} and [2-^{13}C]G_{83}, [1-^{13}C]M_{81} and [2-^{13}C]G_{83}, [1-^{13}C]I_{91} and [2-^{13}C]G_{94}, or [1-^{13}C]I_{95} and [2-^{13}C]G_{98}. In the last peptide, the naturally occurring leucine residue at position 98 was replaced by glycine in order to directly compare the extent of magnetization exchange with the other peptides bearing glycine $^{13}CH_2$ labels. The purity of the peptides was characterized by mass spectroscopy, which revealed protonated molecular ions at *m/e* ratios in agreement with those expected from the sequence and isotopic incorporation. Reverse-phase HPLC was capable of separating peptides differing in molecular weight by one amino acid.

The GPA-TM peptides were reconstituted into ^2H-DMPC (Avanti Polar Lipids, Alabaster, AL) using detergent dialysis. Pure peptide and DMPC were separately dissolved in 2% octyl β-glucoside. They were then combined in a 20:1 lipid to peptide molar ratio using typically 15 mg of peptide and sonicated in 3–5 freeze–thaw cycles. The octyl β-glucoside was dialyzed using Spectra-Por 3 dialysis tubing (3000 MW cutoff) for 1–2 days against phosphate buffer (10 mM phosphate and 50 mM NaCl, pH 7). The samples were then run on a 20–70% sucrose gradient and washed twice with buffer. About two-thirds of the wet sample pellet was transferred into a 5-mm NMR rotor. The remainder was used for CD and IR spectroscopy.

CD spectra were obtained on an AVIV 60DS or 62DS spectrometer in a quartz cuvette of 0.1-mm path length. Repetitive scans were recorded at 28 °C with a 1-s integration time, a 0.5-nm step size, and a 1.5-nm bandwidth. The spectra were collected in phosphate buffer with and without 2.5% octyl β-glucoside. The protein concentration in the CD samples was determined to within 10% by amino acid analysis using two aliquots of each sample. Spectra of peptide-free lipid vesicles prepared in parallel with the lipid–peptide samples were used to correct for background lipid absorbance and scattering.

Polarized ATR-FTIR absorbance spectra were obtained using the GPA-TM peptide incorporated into a single supported DMPC bilayer on a 45° trapezoidal Ge IR-ATR plate. Peptide was incorporated by using the vesicle fusion technique of Tamm and Tatulian (1993). Briefly, a monolayer was prepared on the surface of a circular Fromherz/Langmuir–Blodgett trough (Mayer, Göttingen, Germany) using a compression of 32.2 mdyn/cm. The plasma-cleaned 50 × 20 × 2 mm^3 Ge plate was then rapidly submerged beneath the DMPC monolayer at a speed of 16 cm/min and slowly withdrawn at 6 mm/min to cast the monolayer onto the plate's two main surfaces. Next, the Ge plate was placed into a stainless steel ATR liquid sample holder with PTFE O-rings (Buck Scientific, East Norwalk, CT). DMPC vesicles (0.250 mM) were prepared by sonicating dried lipid in ^2H_2O buffer (10 mM KH_2PO_4, pH 7.3, and 150 mM NaCl) until the solution was optically transparent. These vesicles were then mixed and further sonicated with a portion of a 20:1 DMPC–glycophorin peptide vesicle pellet and additional ^2H_2O buffer until the final lipid and peptide concentrations were ca. 540 and 24 μM, respectively. This vesicle solution was then added to both sides of the ATR liquid sample holder, and the entire assembly was shaken gently for 50 min so that the peptide-containing vesicles could fuse with the supported monolayer. Finally, both liquid compartments were rinsed with 7 vol of the ^2H_2O buffer solution to remove excess vesicles that did not incorporate into the supported bilayers. After data were obtained using the supported DMPC bilayer–GPA-TM sample,

the membrane was removed from the Ge ATR plate by running ethanol through the compartments without moving the ATR plate. The apparatus was then rinsed and filled with the ^2H_2O buffer solution and was used to obtain the background absorbance spectra.

FTIR spectra were obtained using 4-cm^{-1} resolution and two sets of 4000 scans for both sample and background on a Nicolet 740 FTIR spectrometer (Madison, WI). The IR beam was polarized perpendicular or parallel using a 1-in-diam. wire-grid ZnSe polarizer from Optometrix USA, Inc. (Ayer, MA). Peptide and lipid order parameters were calculated using the equations and optical constants of Tamm and Tatulian (1993).

Magic angle spinning NMR experiments were performed on a Chemagnetics CMX 360-MHz spectrometer using a 5-mm high-speed double-resonance probe from Doty Scientific (Columbia, SC). The sample spinning speed for the rotational resonance experiments was kept constant to within 5 Hz using a spinning-speed controller from Doty Scientific. The temperature was maintained at ca. 5 or −50 °C in order to slow residual rotational diffusion of the peptide which might otherwise average the dipolar couplings being measured. The pulse sequence used for the RR NMR experiments has been described previously (Peersen et al., 1992). Briefly, the sequence begins with ^{1}H–^{13}C cross polarization to generate ^{13}C polarization that is then stored on the z-axis with a ^{13}C flip-back pulse. One of the two ^{13}C resonances is selectively inverted with a low-power 500-μs pulse, and magnetization is allowed to exchange between the two sites for a variable mixing period (t_m). The power level of the inversion pulse is carefully adjusted to yield the maximum inversion. The distribution of ^{13}C signal at the end of the mix period is detected with a 90° pulse that flips the magnetization into the transverse plane for acquisition of the NMR signal. Strong ^{1}H decoupling is essential during the variable mix and acquisition periods (Peersen & Smith, 1993). The decoupling power was set to a field strength of 83 kHz during the variable delay and acquisition. This level of decoupling was sufficient to maximize RR exchange as determined by a comparison of exchange rates at different decoupling field strengths.

Conventional single-amplitude CP was replaced by variable-amplitude cross polarization (VACP) for these experiments to enhance the carbon signals at high MAS frequencies and yield more reliable intensities (Peersen et al., 1993, 1994). During the 5-ms CP contact time, the ^{13}C amplitude corresponded to a constant spin-lock frequency of ~70 kHz, while the proton amplitude was varied in nine steps, each 555 ms in length. The first proton amplitude was centered at a B_1 field strength of 70 kHz, and the additional amplitudes were increased or decreased in ~2-kHz steps. The VACP sequence yields stable and reproducible signals that are essential for generating the difference spectra and the magnetization exchange curves used for determining internuclear distances.

RESULTS AND DISCUSSION

CD Spectroscopy. CD measurements are commonly used to assess protein secondary structure. The CD spectrum is analyzed by deconvolution using a basis set of CD spectra corresponding to α-helix, β-sheet, β-turn, and random coil (Johnson, 1990). The interpretation of the CD spectra of membrane proteins is complicated by differential light scattering and differential absorption flattening that can lead to a nonlinear attenuation of the CD bands at strong absorption peaks as well as red shifts in the peak positions (Duysens, 1956; Gordon & Holzwarth, 1971; Urry & Long, 1980; Mao & Wallace, 1984; Glaeser & Jap, 1985; Park et al., 1992). In the past, these features have led to controversy in the estimates of membrane protein secondary structure. A loss of intensity at 190 and 208 nm is often observed in membrane proteins containing α-helical secondary structure and, when coupled to spectral red shifts, is similar to the conversion of α-helix to β-sheet or β-turn.

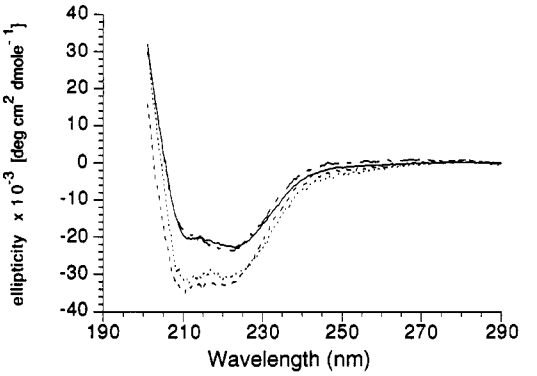

FIGURE 1: CD spectra of the GPA-TM domain. Comparisons are shown between GPA-TM in DMPC at lipid:peptide ratios of 20:1 (—) and 100:1 (···) and GPA-TM at a lipid:peptide ratio of 20:1 (– – –) that has subsequently been solubilized with 5% octyl β-glucoside (- - -). Spectra were taken at 28 °C in pH 7 phosphate buffer.

Figure 1 compares the CD spectra of the GPA-TM peptide reconstituted in DMPC at lipid:protein ratios of 20:1 (—) and 100:1 (···). In both samples, minima are observed at approximately 208 and 222 nm that are characteristic of α-helical structure. Increasing the lipid:protein ratio results in an increase of the CD signal and a more pronounced minimum at 208 nm. Similar CD spectra were obtained on a second 20:1 reconstituted sample (– – –) that has subsequently been solubilized with 2.5% octyl β-glucoside (- - -). The replicate 20:1 samples illustrate the reproducibility of the CD signal in different preparations. The addition of octyl β-glucoside disperses the membrane vesicles, leading to a CD signal comparable to that observed with the 100:1 reconstitution. In general, the content of helix is estimated by the mean residue ellipticity. The apparent ellipticity depends strongly on the lipid to peptide ratio. The favorable comparison between the CD spectra obtained with a 100:1 reconstitution and solubilized with octyl β-glucoside indicates that both dilution and solubilization minimize the optical influences on the CD shape and intensity.

The magnitude of the 208- and 222-nm CD absorbance based on soluble protein data sets is approximately −36 000 ± 3000 deg cm^2 dmol^{-1} (Tinoco et al., 1963; Chen et al., 1974; Park et al., 1992). The observed ellipticity of the GPA-TM peptide in detergent or at high lipid:protein ratios is in the range of 32 000–34 000 deg cm^2 dmol^{-1}, arguing that under these conditions the peptide is 80–100% helical. The 30–40% decrease in CD signal in the 20:1 reconstitution might be interpreted in terms of differential absorption flattening, although loss of helical secondary structure would also be consistent with the data. The situation, however, is complicated by the recent results of Fasman and co-workers (1992), who have deconvoluted the CD spectrum of a "standard" membrane α-helix from a set of detergent-solubilized membrane proteins and found that the magnitudes of the 208- and 222-nm bands are on the order of −50 000 and −60 000 deg cm^2 dmol^{-1}, respectively. This would suggest that a substantial fraction (30–50%) of the GPA-TM peptide, even under optimal conditions, is not helical. Consequently, the only conclusion

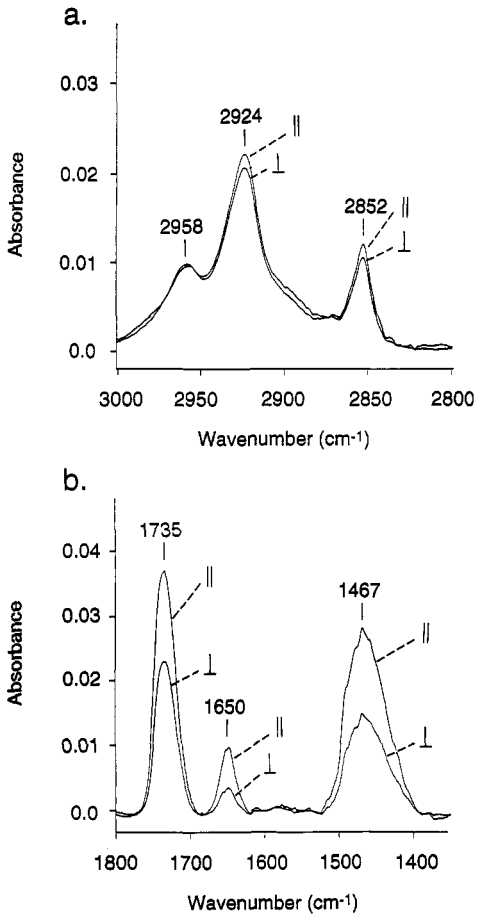

FIGURE 2: (a) Parallel and perpendicular polarized ATR-FTIR absorbance spectra between 3000 and 2800 cm^{-1}. The spectra represent the average of two trials that were added and baseline adjusted without smoothing. Each trial consisted of two sets of 4000 scans of both the DMPC–glycophorin bilayer sample and a D_2O buffer background at each polarization. (b) Parallel and perpendicular polarized ATR-FTIR absorbance spectra between 1800 and 1300 cm^{-1}. The spectra represent the average of two trials that were added and baseline adjusted by a six-point function. A water vapor spectrum was also subtracted.

that can be drawn is that the secondary structure cannot be determined solely by the CD analysis.

ATR-FTIR Spectroscopy. The ATR-FTIR measurements complement and extend the CD data. Symmetric DMPC bilayers formed with the GPA-TM peptide and supported on a Ge ATR plate demonstrated good lipid order in the presence of the peptide when studied by polarized ATR-IR spectroscopy. Figure 2a shows the IR absorbance spectra obtained between 3000 and 2800 cm^{-1} of the DMPC–GPA-TM (24:1) bilayers using perpendicular or parallel polarized light. The peak at 2958 cm^{-1} represents the lipid CH_3 asymmetric stretching vibration. Absorbance maxima at 2924 and 2852 cm^{-1} represent the asymmetric and symmetric lipid CH_2 stretching vibrations, respectively; dichroic ratios and order parameters were calculated using each of these peaks. As seen in Table 1, the averaged dichroic ratios for the 2924 and 2852 cm^{-1} absorbances are 1.08 and 1.09, respectively. The resulting averaged order parameters, S_{lipid}, for the 2924 and 2852 cm^{-1} peaks are 0.68 and 0.67, respectively. These results indicate that a well-ordered lipid bilayer is formed parallel to the ATR plate surface in the presence of the peptide. These data are similar to those obtained by Frey and Tamm (1991) using an asymmetric POPC/POPG/POPC bilayer with incorporated melittin.

Table 1: Calculated Values of Dichroic Ratios, R, and Order Parameters for the Amide I Peak at 1650 cm^{-1}, S_{helix}, and the Lipid CH_2 Stretching Peaks at 2924 and 2852 cm^{-1}, S_{lipid}[a]

	2924 cm^{-1}	2852 cm^{-1}	1650 cm^{-1}
dichroic ratio	1.08	1.09	2.14
order parameter	+0.68[b]	+0.67[b]	+0.35[c]

[a] Averaged spectral data pertaining to these calculations are shown and described in Figure 2. [b] S_{lipid}. [c] S_{helix}/S_{lipid}.

Figure 2b shows the IR absorbances obtained for the supported DMPC–GPA-TM bilayer between 1400 and 1800 cm^{-1}. In this region, amide I and amide II absorbances are seen at 1650 and ~1467 cm^{-1}, respectively. The peak at 1735 cm^{-1} is the lipid C=O stretching vibration. The amide absorbances are those expected for an α-helical conformation in ^2H_2O; the lack of significant absorbance at 1550 cm^{-1} indicates complete H/D exchange. The average dichroic ratio of the 1650 cm^{-1} ATR absorbances is 2.14 (Table 1). Using this result, the helical order parameter, S_{helix}, is calculated to be $0.35/f_{helix}$, where f_{helix} is the fraction of the α-helix in the peptide. On the basis of the CD data, the fraction of helix can lie anywhere between 50 and 100%. However, the observed IR spectrum of the peptide in the bilayer shows most amide I intensity at 1650 cm^{-1}, as expected for a predominantly α-helical structure. Furthermore, as discussed below, the NMR data argue for a helical content of ~70%, giving an order parameter of 0.5. This indicates that the helix orientation is more perpendicular (transmembrane) than parallel to that of the membrane surface. The result is clearly different from that obtained by Tamm and Tatulian (1993), who found helical order parameters for wild-type signal peptides of glucitol (22 amino acids) and mannitol (23 amino acids) PTS permeases to be ~–0.50 in single supported bilayers. Frey and Tamm (1991) also found that the helical order parameter for melittin (26 amino acids) in single supported lipid bilayers and ^2H_2O buffer was ~ –0.50. The helical order parameter of –0.50 indicated that both of the signal peptides and mellitin in the supported bilayers aligned parallel to the membrane surface.

Intrahelical RR NMR Measurements. Accurate internuclear distance measurements along the length of the transmembrane sequence provide a way to directly establish the type and amount of secondary structure. Figure 3 shows the region of the GPA-TM domain between L_{75} and L_{89} and indicates two of several intramolecular distances that are sensitive to the secondary structure of the peptide. The internuclear distances predicted from the helical model are 4.4 Å between the α-carbon of G_{83} and the backbone carbonyl of V_{80} across one turn of the helix and 4.4 Å between the α-carbon of G_{83} and the backbone carbonyl of M_{81} roughly across the diameter of the helix (Treutlein et al., 1992). These distances are considerably longer in nonhelical geometries.

Figure 4 presents the ^{13}C MAS NMR spectra of the unlabeled GPA-TM peptide (b) and a peptide that has been ^{13}C-labeled at the α-carbon of G_{83} and the backbone carbonyl of V_{80} (a). The ^{13}C-labeled peptide is designated GPA-TM [V_{80}–G_{83}]. Both peptides have been reconstituted into [^2H]-DMPC at a 20:1 lipid to peptide molar ratio. Deuteration of the lipid removes most of the natural abundance ^{13}C signal of the acyl chains in the ^1H–^{13}C cross-polarization experiment by eliminating the ^1H spins, although a substantial component of the residual natural abundance intensity comes from lipid $^{13}CD_2$ groups that cross polarize from protons of the peptide. Comparison of the two spectra allows easy assignment of the ^{13}C-labeled backbone carbonyl of V_{80} and α-carbon of G_{83} to the resonances at 175 and 44 ppm, respectively. Figure 5

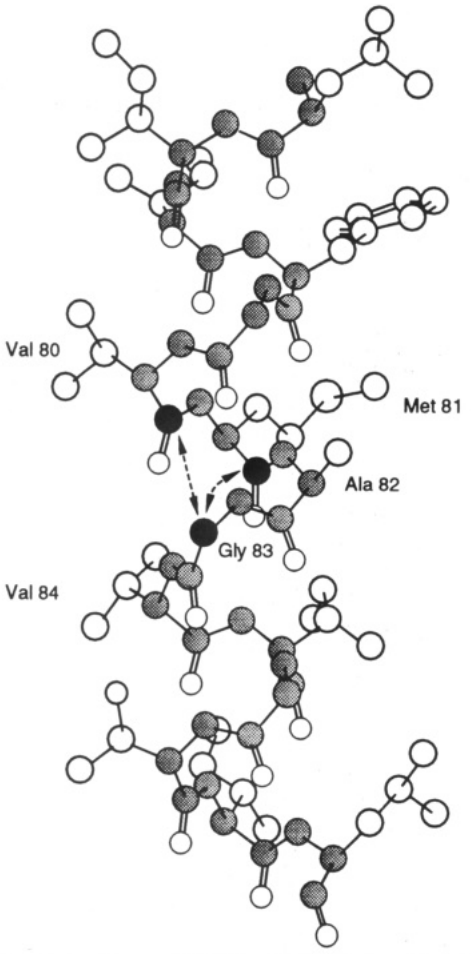

FIGURE 3: Molecular model of the GPA-TM domain between L_{75} and L_{89} showing the intrahelical distances between ^{13}C labels in the GPA-TM [V_{80}–G_{83}] and GPA-TM [M_{81}–G_{83}] peptides. The arrows connect the labeled carbons across the diameter ($V_{80} \Leftrightarrow G_{83}$) and one turn of the α-helix ($M_{81} \Leftrightarrow G_{83}$).

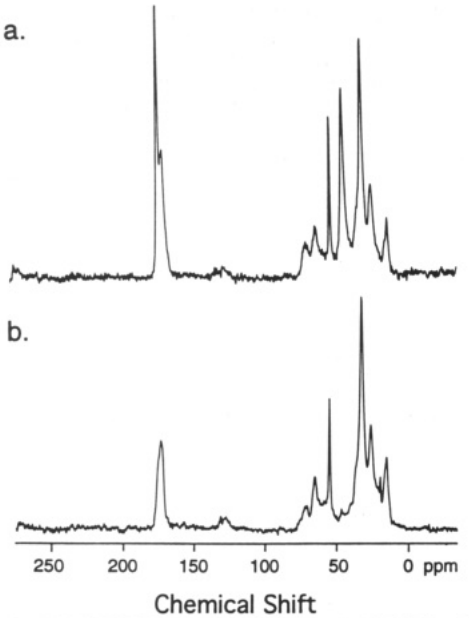

FIGURE 4: MAS NMR spectra of (a) GPA-TM [V_{80}–G_{83}] incorporating ^{13}C labels at [1-^{13}C]V_{80} and [2-^{13}C]G_{83} and (b) unlabeled GPA-TM. The peptides were reconstituted at a 20:1 lipid to peptide ratio into [^2H]DMPC. The labeled signals are clearly observed at 175 and 44 ppm.

presents RR NMR spectra of GPA-TM [V_{80}–G_{83}]. The $^{13}C{=}O$ resonance has been selectively inverted with a 500-μs pulse. The top spectrum was obtained at a short mix time (1 ms) such that significant exchange has not yet occurred, and the additional spectra show exchange after mixing times of 10, 20, and 40 ms. A decrease in the intensity of the $^{13}C{=}O$ resonance is clearly coupled to a decrease in the $^{13}CH_2$ intensity. These spectra were obtained at the $n = 1$ resonance condition by spinning the sample at 11 830 Hz, corresponding to the frequency separation between the $^{13}CH_2$ and $^{13}C{=}O$ peaks in the MAS spectrum.

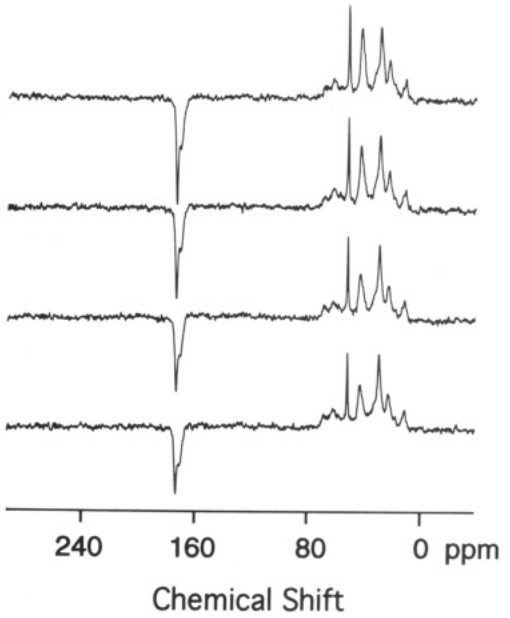

FIGURE 5: ^{13}C RR NMR spectra of the GPA-TM [V_{80}–G_{83}] peptide in deuterated DMPC bilayers. The specific ^{13}C labels on Gly 83 [$^{13}CH_2$] and Val 80 [$^{13}C{=}O$] are estimated to be ~4.4 Å apart in the α-helical model of glycophorin (Treutlein et al., 1992). The spectra were obtained at a MAS frequency of 11 830 ± 5 Hz. The temperature was maintained at −50 °C. Spectra were obtained with mixing times, from top to bottom, of 1, 10, 20, and 40 ms. Each spectrum is the average of 1024 scans using ~10 mg of peptide.

The $n = 1$ magnetization exchange curves of the four peptides studied are presented in Figure 6 along with simulations for a $CH_2 \Leftrightarrow C{=}O$ spin pair at different internuclear distances. The experimental intramolecular magnetization exchange curves were generated by integration of the $^{13}CH_2$ and $^{13}C{=}O$ peaks in the RR NMR spectra. Due to the strong proton couplings in the $^{13}CH_2$ group, the influence of high-speed MAS on CP efficiency is minimal. This is not the case for the $^{13}C{=}O$ group that has no directly bonded protons and exhibits large oscillations in its Hartmann–Hahn matching profile at high MAS frequencies (Peersen et al., 1993). One of the advantages of the VACP sequence is that the Hartmann–Hahn profile for the $^{13}C{=}O$ resonance is broadened to resemble that of the $^{13}CH_2$ group. This results in more stable intensities over the course of the RR NMR experiment. A comparison of the simulated curves and the scatter in the experimental data points shows that the precision in these measurements is about 0.2 Å.

The natural abundance intensity contributing to each resonance was determined by integration of a spectrum of the reconstituted unlabeled GPA-TM peptide. Since we typically observe an oscillation in the intensity of the time points below ~1 ms, possibly due to probe ringdown, the intensities of the first three time points (100 μs, 500 μs, and 1 ms) have been averaged and normalized to a value of 1.0. Several off rotational resonance data points are also shown in Figure 6a. The off-RR curve provides a baseline for quantitating the extent of RR-driven exchange. The lipid CH_2 (30 ppm) and

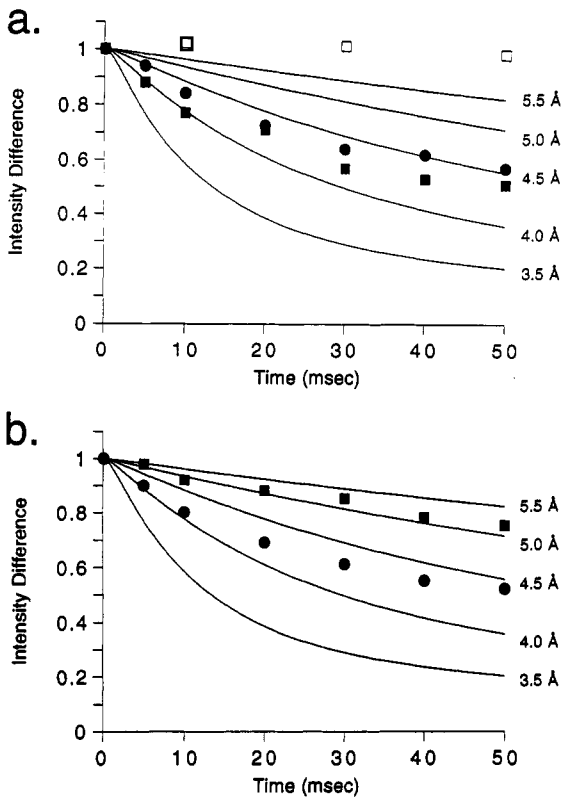

FIGURE 6: (a) Magnetization exchange curves and simulations for GPA-TM [V_{80}–G_{83}] (●) and GPA-TM [M_{81}–G_{83}] (■) along with several off rotational resonance (□) data points. (b) Magnetization exchange curves and simulations for GPA-TM [I_{91}–G_{94}] (●) and GPA-TM [I_{95}–G_{98}] (■). The simulated exchange curves were generated using a fixed 0.8-ms zero-quantum T_2 and varying only the dipolar coupling to obtain different distances.

choline methyl (55 ppm) resonances appear to be more sensitive to temperature changes than the protein resonances and can exhibit intensity changes that are not associated with the RR-driven exchange. We show in the preceding paper that the lipid line widths are sensitive to temperature (Smith et al., 1994) to a much greater extent than the peptide resonances in this study.

Simulations of the magnetization exchange curves were performed using the methods of Levitt et al. (1990). Several parameters must be defined for these calculations. The chemical shift tensors for the C=O and CH_2 groups are taken from studies on alanylalanine and glycine, respectively (Haberkorn et al., 1981; Hartzell et al., 1987; Oas et al., 1987). The relative shift tensor orientations cannot be defined without assuming a secondary structure. However, this is not a problem for the $n = 1$ exchange curves, which are not sensitive to the tensor orientations (Levitt et al., 1990). The two parameters that dominate the calculated exchange rates are the dipolar coupling, which is related to the internuclear distance, and the zero-quantum T_2 relaxation. The value of the dipolar coupling was varied in the simulations to correspond to distances between 3.5 and 5.5 Å. The zero-quantum T_2 was estimated from the observed line widths (Δ) to be ~800 μs using the relationship $T_2 = 1/\pi(\Delta C{=}O + \Delta CH_2)$. Using this value for the zero-quantum relaxation, the simulations for the GPA-TM [V_{80}–G_{83}], GPA-TM [M_{81}–G_{83}], and GPA-TM [I_{91}–G_{94}] peptides yield estimates of the internuclear distance of 4.0–4.5 Å, close to the value expected for helical structures. The natural line widths in these samples may be narrower than the observed line widths due to conformational heterogeneity, and consequently 800 μs is likely to be an underestimate of the zero-quantum T_2. A longer T_2 would result in a longer estimate for the internuclear distance.

An alternative approach for estimating internuclear distances from the experimental magnetization exchange curves is by comparison of the exchange rates with those determined from crystalline samples where the internuclear distances are known independently from a crystal structure. We have shown that such comparisons yield accurate backbone carbonyl to alanine CH_3 distances in alamethicin peptides reconstituted into membrane bilayers (Peersen et al., 1992). These crystal–membrane comparisons serve as controls to show how the RR exchange curves change as a function of internuclear distance.

Comparison of the GPA-TM exchange rates with rates corresponding to known distances of 3.7–6.8 Å in crystalline alamethicin peptides (Peersen et al., 1992; O. B. Peersen, S. Aimoto, and S. O. Smith, in preparation) indicate that the ^{13}C labels are ~5 Å apart in the GPA-TM [V_{80}–G_{83}], GPA-TM [M_{81}–G_{83}], and GPA-TM [I_{91}–G_{94}] peptides. However, this direct comparison is not completely valid because the glycine CH_2 label in GPA-TM peptides has much stronger proton couplings than the alanine CH_3 labels used in the alamethicin, and this may lead to a difference in the zero-quantum relaxation term even though 83-kHz proton decoupling was used in each experiment. If the distances were identical, then the CH_2 transfer rate may be slower than that of the CH_3 group because of a shorter zero-quantum T_2. As a result, the ~5-Å estimate obtained by the comparison is an *upper* limit on the distance in GPA-TM. Taken together, the simulations and exchange curve comparisons suggest internuclear separations in these first three GPA-TM peptides of 4.5 ± 0.5 Å. The distance between corresponding α-carbons and carbonyl carbons in the transmembrane segments of the crystal structure of the photosynthetic reaction center proteins from *Rhodopseudomonas viridis* is on average ~4.5–4.6 Å (Deisenhofer et al., 1987).

These results indicate that the secondary structure of glycophorin A transmembrane domain is helical through residue 94. This contrasts with the conclusions of Welsh et al. (1985) on the basis of CD measurements that the stretch of amino acids from L_{90} to Y_{93} adopts a β-strand conformation. The residues S_{92}-Y_{93}-G_{94} are predicted to have a high conformational preference for β-structures [e.g., see Levitt (1978)]; however, most studies on amino acid distributions have been based on soluble proteins and may not fully reflect the conformational preferences in membranes. In a similar fashion, glycine residues often disrupt helical secondary structure in soluble proteins yet clearly do not influence the local secondary structure in the GPA-TM peptide, in part because the hydrogen bonds along the helical backbone are stabilized in the hydrophobic interior of the membrane.

In contrast, the magnetization exchange curve of GPA-TM [I_{95}–G_{98}] indicates a much longer internuclear distance of 5.0–5.5 Å. These labels are much closer to the C-terminus of the peptide and consequently the membrane interface. We substituted a glycine residue at position 98 for the naturally occurring leucine in order to directly compare the results with those from the other three peptides discussed above having a backbone $^{13}C{=}O$ label at residue i and a $^{13}CH_2$ label at residue $i + 3$. Despite the glycine substitution at this position, the CD spectrum of the peptide is not altered (data not shown). The longer distance obtained by the RR measurement indicates that the helical structure observed in the interior of the protein begins to unravel at the membrane interface. A loss of helical structure in the last four residues at both the N- and C-terminal ends of the 29-residue peptide should result in a loss of ~30%

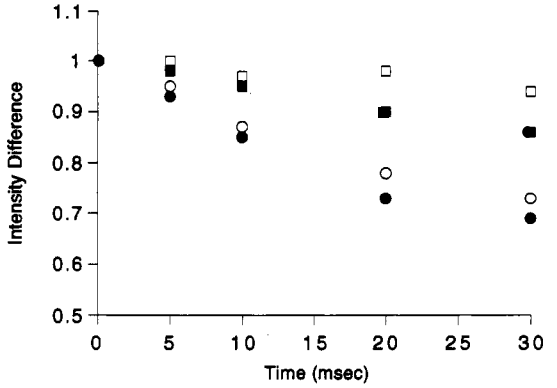

FIGURE 7: Magnetization exchange curves for GPA-TM [I_{91}–G_{94}] (●, ○) and GPA-TM [I_{95}–G_{98}] (■, □) at −50 °C (filled symbols) and 5 °C (open symbols). The data were obtained at the $n = 2$ resonance condition.

in the helical CD signal. This would argue that the mean residue ellipticity is on the order of 46 000–49 000 deg cm^2 dmol^{-1}. The higher value estimated for the mean residue ellipticity of transmembrane α-helices is consistent with the conclusions of Fasman and co-workers (Park et al., 1992). Further studies are possible to test whether the length of the peptide influences the secondary structure at the membrane interface.

Finally, RR NMR measurements were made at 5 °C on the GPA-TM [I_{95}–G_{98}] and GPA-TM [I_{91}–G_{94}] peptides in order to characterize peptide structure and mobility at a higher temperature; the NMR data discussed above were obtained at −50 °C to ensure that the peptide was rigid and the full dipolar couplings were observed in the RR NMR experiment. Both temperatures are well below the DPPC phase-transition temperature of 42 °C. Previous experiments on DPPC alone over the −50 to 5 °C temperature range showed no significant difference in the RR exchange curves, suggesting no large changes in lipid structure (Smith et al., 1994). The higher temperature would only be expected to influence mobile groups surrounded by bulk water at the membrane interface. Figure 7 presents magnetization exchange curves for the GPA-TM [I_{95}–G_{98}] and GPA-TM [I_{91}–G_{94}] peptides at −50 °C and 5 °C. These data were obtained at the $n = 2$ resonance condition; MAS experiments at the $n = 1$ resonance condition ($\sim$11 800 Hz) at 5 °C were not undertaken due to problems associated with spinning fully hydrated multilayers at high MAS speeds. Comparison of the magnetization exchange curves obtained at −50 and 5 °C for the GPA-TM [I_{91}–G_{94}] peptide indicates that the helical peptide structure is maintained at the higher temperature. However, comparison of the exchange curves for the GPA-TM [I_{95}–G_{98}] peptide shows a slight decrease in magnetization exchange at 5 °C suggesting that this region of the peptide is more mobile and/or less structured at this temperature. Experiments are in progress to more completely characterize the influence of dynamics on the observed RR exchange rates. Motional averaging of the dipolar interaction will decrease magnetization exchange and lead to a longer estimate of the internuclear distance. In general, it will be necessary to determine the extent of motional averaging in RR measurements in membrane systems by measuring the exchange rate between ^{13}C sites at known (or relatively fixed) distances in the molecule under study.

CONCLUSIONS

In this paper, we have combined CD and IR spectroscopy to characterize the global secondary structure and orientation of the transmembrane domain of glycophorin, and explored the use of rotational resonance NMR for characterizing local secondary structure through the measurement of internuclear distances. The NMR results demonstrate that distance measurements can be made with high resolution in a membrane environment. These studies represent the first step of a possible approach for determining the structure of integral membrane proteins in lipid bilayers in which one first establishes the secondary structure of the transmembrane sequences and subsequently determines the tertiary interactions between these domains and with the surrounding lipids.

ACKNOWLEDGMENT

We gratefully acknowledge Dr. Raj Betageri for the t-Boc chemistry, Günther Metz for obtaining the CD data, and Shy Arkin, Brian DeDecker, John Hunt, Sarah Keill and Mark Lemmon for assistance at various stages of peptide purification and reconstitution. We thank Don Engelman, Axel Brünger, Herbert Treutlein and Paul Adams for invaluable discussions, and Malcolm Levitt and Bob Griffin for the original and updated version of the CC2Z simulation program. We also thank Lukas Tamm and Suren Tatulian for advice and assistance in making supported bilayer films.

REFERENCES

Bormann, B. J., & Engelman, D. M. (1992) *Annu. Rev. Biophys. Biomol. Struct. 21*, 223–242.
Bormann, B. J., Knowles, W. J., & Marchesi, V. T. (1989) *J. Biol. Chem. 264*, 4033–4037.
Chen, Y., Yang, J. T., & Chau, K. H. (1974) *Biochemistry 13*, 3350–3359.
Deisenhofer, J., Epp, O., Miki, K., Huber, R., & Michel, H. (1987) *Nature 318*, 618–624.
Duysens, L. N. M. (1956) *Biochim. Biophys. Acta 19*, 1–12.
Farrar, M. R., Laksmi, K. V., Smith, S. O., Brown, R. S., Raap, J., Lugtenburg, J., Griffin, R. G., & Herzfeld, J. (1993) *Biophys. J. 65*, 310–315.
Frey, S., & Tamm, L. (1991) *Biophys. J. 60*, 922–930.
Furthmayr, H., & Marchesi, V. T. (1976) *Biochemistry 15*, 1137–1144.
Glaeser, R. M., & Jap, B. K. (1985) *Biochemistry 24*, 6398–6401.
Gordon, D. J., & Holzwarth, G. (1971) *Arch. Biochem. Biophys. 142*, 481–488.
Haberkorn, R. A., Stark, R. E., van Willigen, H., & Griffin, R. G. (1981) *J. Am. Chem. Soc. 103*, 2534–2539.
Hartzell, C. J., Whitfield, M., Oas, T. G., & Drobny, G. P. (1987) *J. Am. Chem. Soc. 109*, 5966–5969.
Johnson, W. C., Jr. (1990) *Proteins 7*, 205–214.
Kubo, A., & McDowell, C. A. (1988) *J. Chem. Soc., Faraday Trans. 1: 84*, 3713–3730.
Lemmon, M. A., Flanagan, J. M., Hunt, J. F., Adair, B. D., Bormann, B. J., Dempsey, C. E., & Engelman, D. M. (1992a) *J. Biol. Chem. 267*, 7683–7689.
Lemmon, M. A., Flanagan, J. M., Treutlein, H. R., Zhang, J., & Engelman, D. M. (1992b) *Biochemistry 31*, 12719–12725.
Levitt, M. (1978) *Biochemistry 17*, 4277–4284.
Levitt, M. H., Raleigh, D. P., Creuzet, F., & Griffin, R. G. (1990) *J. Chem. Phys. 92*, 6347–6364.
Mao, D., & Wallace, B. A. (1984) *Biochemistry 23*, 2667–2673.
Oas, T. G., Hartzell, C. J., McMahon, T. J., Drobny, G. P., & Dahlquist, F. W. (1987) *J. Am. Chem. Soc. 109*, 5956–5962.
Park, K., Perczel, A., & Fasman, G. D. (1992) *Protein Sci. 1*, 1032–1049.
Peersen, O. B., & Smith, S. O. (1993) *Concepts in Magn. Reson. 5*, 305–317.
Peersen, O. B., Yoshimura, S., Hojo, H., Aimoto, S., & Smith,

S. O. (1992) *J. Am. Chem. Soc. 114*, 4332–4335.
Peersen, O. B., Wu, X., Kustanovich, I., & Smith, S. O. (1993) *J. Magn. Reson. 104*, 334–339.
Peersen, O. B., Wu, X., & Smith, S. O. (1994) *J. Magn. Reson. 106*, 127–131.
Raleigh, D. P., Levitt, M. H., & Griffin, R. G. (1988) *Chem. Phys. Lett. 146*, 71–76.
Roeske, R. (1963) *J. Org. Chem. 28*, 1251–1253.
Smith, S. O., Hamilton, J., Salmon, A., & Bormann, B. J. (1994) *Biochemistry* (preceding paper in this issue).
Tamm, L. K., & Tatulian, S. A. (1993) *Biochemistry 32*, 7720–7726.
Thompson, L. K., McDermott, A., Raap, J., van der Wielen, C.M., Lugtenburg, J., Herzfeld, J., & Griffin, R. G. (1992) *Biochemistry 31*, 7931–7938.
Tinoco, I., Woody, R. W., & Bradley, D. F. (1963) *J. Chem. Phys. 38*, 1317–1325.
Treutlein, H. R., Lemmon, M. A., Engelman, D. M., & Brünger, A. T. (1992) *Biochemistry 31*, 12726–12733.
Urry, D. W., & Long, M. M. (1980) In *Membrane Physiology* (Andreoli, T. E, Hoffman, J. F., & Fanestil, D. D., Eds.) pp 107–124, Plenum, New York.
Welsh, E. J., Thom, D., Morris, E. R., & Rees, D. A. (1985) *Biopolymers 24*, 2301–2332.